

# Effect of Thickness-to-Chord Ratio and Chord Length on Aerodynamics of GOE-387 Airfoil

<sup>1</sup>\*Nazaruddin Sinaga, <sup>2</sup>Bambang Yuniyanto, <sup>3</sup>Yosia Verse Pirie

<sup>1,2,3</sup>Department of Mechanical Engineering, Faculty of Engineering, Diponegoro University, Jl. Prof. Sudharto, SH., Tembalang, Semarang 50275, Indonesia

\*Corresponding Author's E-mail: [nsinaga19.undip@gmail.com](mailto:nsinaga19.undip@gmail.com)

**Abstract** - This research presents CFD analysis of the two-dimensional subsonic flow over a GOE-387 airfoil at various thickness-to-chord ratios ( $t/C$ ) and chord lengths, operating at a Reynolds number of 400,000. Lift Coefficient ( $C_L$ ), Drag Coefficient ( $C_D$ ), and  $C_L/C_D$  are investigated. The geometry of the airfoil is created using SolidWorks and Ansys Design Modeler. CFD analysis uses Ansys Fluent at various  $t/C$  from 5% to 25%, while the chord length varies from 100 to 200 cm. It was shown that variations in chord length have an effect in the form of increases and decreases in the value of the  $C_L$  and a decrease in the  $C_L/C_D$  ratio, which is caused by the greater length value of the GOE-387 airfoil chord. In addition, variations in the thickness-to-chord ratio parameter also clearly influence the aerodynamic characteristics of GOE-387 airfoil. The greater the  $t/C$ , the more significant the lift and drag coefficients increase while the  $C_L/C_D$  ratio decreases.

**Keywords:** Airfoil, lift coefficient, drag coefficient, thickness-to-chord ratio.

## I. INTRODUCTION

Airplane is one type of transportation that can lift heavy loads in the air. This happens because of the lift force generated by the aircraft's wings [1]. An airfoil is defined as the cross-sectional shape of the wing. Its main purpose is to generate lift to carry the aircraft's weight. The force parallel to the relative direction of motion is defined as drag, and the force perpendicular to the direction of motion is defined as lift. Therefore, the airfoil's shape directly affects the wing's aerodynamic performance. The lift-to-drag ratio is one of the most important parameters for wings. Less thrust can achieve significant lift [2].

Optimizing aerodynamic shape is very important with the rapid development of aerospace science and mechanical engineering. The parametric method in aerodynamic form is important in the optimized airfoil optimization process. A well-parameterized method with fewer design parameters can handle larger wing deformations in the design space [3]. To improve the aerodynamic performance of an airfoil, the lift

force is increased, and the drag force is decreased so that the  $C_L/C_D$  ratio is maximized [4].

Aerodynamic shape optimization is carried out to improve aerodynamic performance by modifying the shape or geometry. In a study conducted by Jackson Wozniak [5], which examined the optimization of the geometry and angle of attack of the airfoil to maximize take-off capability, it was found that different geometric parameters, namely the maximum camber position, affect the size of the lift force coefficient. In addition, research in 2021 conducted by Othman and Al-Obaidi [6] regarding the effect of wing airfoil shape on the aerodynamics and performance of jet-trainer aircraft provides aerodynamic data of different airfoil shapes used to determine the aerodynamic characteristics and performance of aircraft for different airfoil shapes.

Apart from the geometric shape of the airfoil itself, the angle of attack adjustment can also affect the aerodynamic characteristics of the airfoil. A study was conducted in 2020 by Gv and Dođru [2] regarding the optimization of airfoils to obtain a research result; namely, the  $C_L/C_D$  ratio of NACA 0012 airfoils has optimal values at angles of attack of 50°, 100° and 150° with an increase of 5% and 10%. To reduce resistance/drag on the airflow on the wings of the aircraft and prevent the formation of vortices, the tips of the wings of the aircraft are fitted with winglets. In 2017, Setyo Hariyadi [7] analyzed the aerodynamic performance of NACA 23018 at cant angles. This study shows the flow characteristics resulting from using winglets where the lift and drag forces increase with an increase in the angle of attack.

## II. BASIC THEORY

Wings are the key aerodynamic structures of an airplane that allow the aircraft to fly. The accessible literature emphasizes the techniques applied to airfoils to achieve the desired augmentation of the lift-to-drag ratio and the delay of flow separation by varying the airfoil structure. The pressure distribution around the airfoil determines the lift and drag forces. The pressure difference between airfoils under different boundary conditions comes from Bernoulli's

principle [5]. For every two points in the irrotational flow field, this can be seen in equation 1.

$$p + \frac{1}{2}\rho V^2 = \text{const} \quad (1)$$

Where  $p$  is pressure,  $\rho$  is density, and  $V$  is velocity. The physical significance of Bernoulli's principle is that when speed increases, pressure decreases, and when speed decreases, pressure increases. Bernoulli's principle illustrates how fluid velocity can generate lift.

From an aerodynamic perspective, the main aircraft lift source is the wings. Therefore, wing shape and size are important for aerodynamic characteristics [8]. A straight line passing through the leading and trailing edges is called a chord line. The straight line distance between the leading and trailing edges is the chord. In the case of a symmetrical shape, the top and bottom surface airfoil geometries are identical so that the mean chamber line is collinear with the chord line [9].

Wing thickness plays an important role in determining the overall performance and characteristics of the air vehicle. The effect of thickness on the aerodynamic characteristics and flow structure over the airfoil has been investigated in the literature. The largest lift coefficient was observed for the thinnest airfoils, but the stall angle of attack was higher for the thicker airfoils. However, the thinnest airfoils have a higher drag coefficient up to the angle of attack [10].

In fluid dynamics, the angle of attack (AOA or  $\alpha$ ) is the angle between the reference line on the body, often the chord line of the airfoil, and the vector representing the relative motion between the body and the fluid through which it travels. The angle of attack is the angle between the body's reference line and the oncoming stream. This article focuses on the most common applications, such as the angle of attack wings or airfoils moving through the air.

As the airfoil moves through the air, the air exerts lift and drag on the airfoil. The lift and drag forces are caused by wall shear and pressure stresses. The lift coefficient can be defined as the ratio of the lift pressure to the dynamic pressure, while the lift pressure is the ratio of the lift to the reference area. The lift force generated by the airfoil depends on its density and relative speed. So, the lift force equation and lift coefficient can be seen in equations 2 and 3.

$$L = \frac{1}{2}\rho U^2 SC_L \quad (2)$$

$$C_L = \frac{L}{\frac{1}{2}\rho v^2 S} = \frac{2L}{\rho v^2 S} = \frac{L}{qS} \quad (3)$$

$L$  is the lift force,  $\rho$  is the air density,  $U$  is the relative velocity,  $S$  is the airfoil area, and  $CL$  is the lift coefficient.

An aircraft's performance through aerodynamic influences is related to fuel consumption, which means that the higher the drag, the greater the resistance received so the fuel consumption will be even greater. In this case, fuel consumption can be reduced by designing a vehicle that maintains good aerodynamics to minimize drag. This drag force is the total drag force in the Z-direction shape used for CD calculations [11]. The drag coefficient of the airfoil also includes the resistance effect caused by the lift. The drag coefficient of a complete structure such as an airplane also consists of the impact of interference drag [12]. Drag force and drag coefficient can be calculated by equations 4 and 5.

$$D = \frac{1}{2}\rho U^2 SC_D \quad (4)$$

$$C_D = \frac{2F_D}{\rho v^2 A} \quad (5)$$

$D$  is the drag force,  $\rho$  is the air density,  $U$  is the relative velocity,  $S$  is the airfoil area, and  $CD$  is the drag coefficient. If the vehicle's  $CD$  is smaller, the fuel consumption will be lower, and performance will be greater. Each car is expected to have a lower  $CD$  because it is influenced by the value of the drag force received by the vehicle. This is because the flow resistance obtained by the car at a certain current speed will be smaller if the resulting drag force is smaller, so it will affect the drag coefficient.

### III. METHODOLOGY

This study will perform a 2D analysis of the airfoil using ANSYS Fluent. Using SolidWorks software, the first step is to make a 3D model of the GOE-387 airfoil with parameter variations such as chord length and a certain thickness-to-chord ratio, as shown in Figure 1.

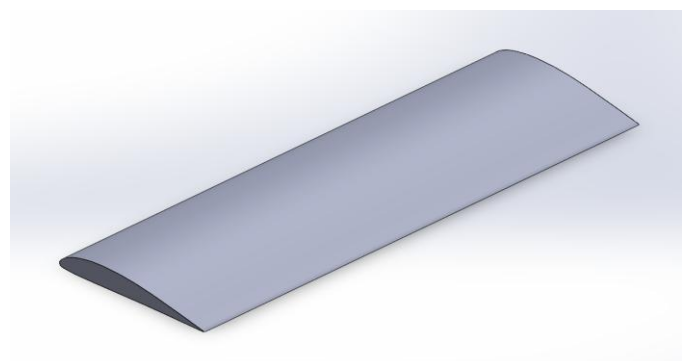


Figure 1: Airfoil 3D Model

In the CFD simulation test, the effect of two geometry variations will be tested, namely chord length and thickness to chord ratio, with the number of variations for each geometry parameter as many as five values, as shown in Table 1 below.

**Table 1: Variation of Test Parameter Values**

Parameter	Value
Chord length	100 cm, 125 cm, 150 cm, 175 cm, 200 cm
Thickness-to-chord ratio	5%, 10%, 15%, 20%, 25%

The airfoil model that was created previously was imported into the Ansys software and converted into a 2D model. In this model, a surface is created around the 2D airfoil model representing the volume. This volume is created by semicircular shapes connected to rectangles. By using Boolean operations, a representative surface is generated between the flow system and the airfoil.

After creating the geometry model, the next step is the meshing process. The mesh must be set to the previous surface, representing the airflow around the airfoil. The mesh is an important part of the simulation because the finer the mesh, the more accurate the simulation. Therefore, the mesh must be finer than the rest throughout the flow domain to understand the aerodynamic behavior along the airfoil. The section to be carried out in the meshing procedure is divided into two sections, with a body of influence along the stream adjacent to the airfoil. This area will affect the mesh density of the body it covers but will not be part of the model geometry, nor will it be merged. The successfully meshed geometry can be seen in Figure 2.

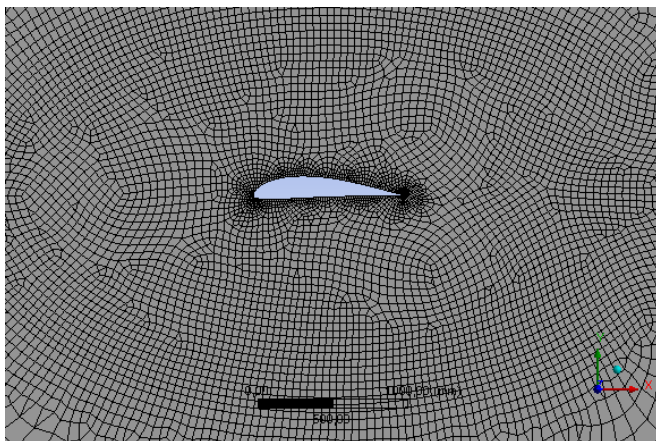


**Figure 2: Meshing Results**

In the meshing process, each edge of the geometric model is named a boundary element. This is done to facilitate the application of boundary conditions in Ansys Fluent [13]. Boundary elements are called the left, top, and bottom sides as inlets, the right side as outlets, and the airfoil edges as airfoil.

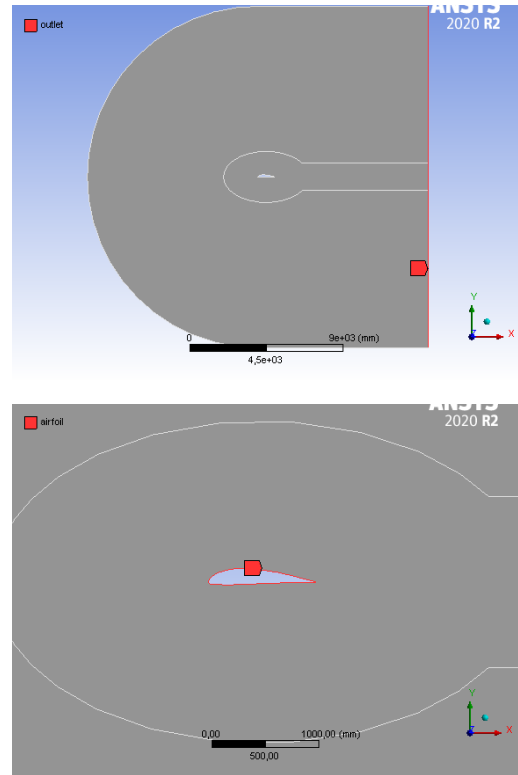


**Figure 2: Boundary Conditions**

The 2D model created in SolidWorks software, edited in the Design Modeler and then developed as a mesh will be used for simulation using ANSYS Fluent, as shown in Figure 3. The simulation phase is carried out through several stages that must be carried out such as the following:

1. The setting stage of the dense model type. The viscous model used is transition-k-kl-omega, which conforms to calculations made in the reference literature.
2. Material type selection stage. This is done by adding the type of fluid used for the simulation and entering the property values of the fluid used.
3. The boundary condition setting stage. Boundary conditions will be given to each predetermined boundary element, including inlet, outlet, and airfoil. Boundary elements, as shown in Figure 3, in the form of inlets will be classified as velocity inlets, boundary elements in the form of outlets will be classified as pressure outlets, and boundary elements in the form of airfoils will be classified as walls with no-slip conditions.
4. The stage of entering the reference value used to obtain the simulation results.
5. The stage of determining the solution method. The method used by the scheme is coupled by activating the pseudo-transient option.
6. The stage of determining the desired output data generated via report definitions.
7. Initialization stage, using hybrid initialization.

- The calculation phase begins by determining the number of iterations needed. The calculation process can be run after all the settings and setup are complete.

#### IV. RESULTS AND DISCUSSIONS

A validation process must be carried out to determine whether the simulation results match the physical reality. Validation is carried out by comparing the results of the lift coefficient obtained based on the simulation with the lift coefficient obtained in the reference literature. The same airfoil geometry was used in the validation as in the reference literature: the GOE-387 airfoil with an angle of attack of 0° and a chord length of 1 m. This validation will also apply the same simulation procedure and compare the lift coefficient results.

After the simulation, convergent results were obtained at the 72<sup>nd</sup> iteration. The lift coefficient obtained from the simulation is 0.4932, while the reference literature has a lift coefficient of 0.5143. The following is a calculation to determine the percentage difference in the lift coefficient results.

$$\Delta C_L = \frac{0.5143 - 0.4932}{0.5143} \times 100\%$$

A difference value of 4.1027% or below 5% is obtained based on validation calculations. Therefore, this shows that this simulation has been validated with results close to those of the reference literature.

From the result of the simulations on the thickness-to-chord ratio parameter, an overview of the condition of the airflow velocity in the area around the airfoil is obtained with variations in the thickness-to-chord ratio of 5%, 10%, 15%, 20%, and 25% with fixed chord length. The contour of velocity from the simulation with geometric parameters in the t/C ratio is shown in Figures 4 to 8.

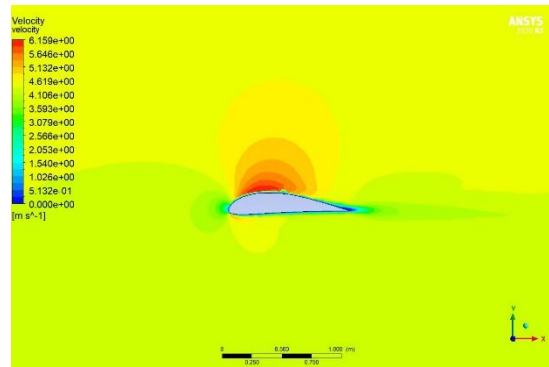


Figure 5: Velocity contour for t/C ratio of 15%

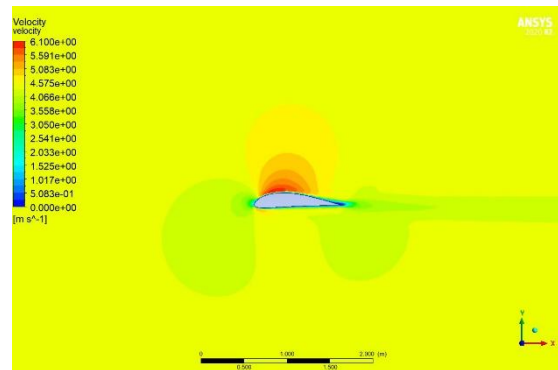


Figure 6: Velocity contour for t/C ratio of 10%

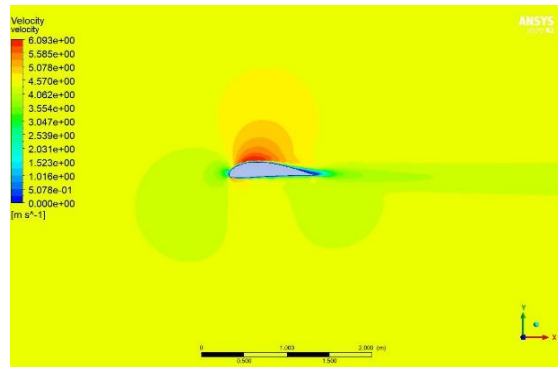


Figure 7: Velocity contour for t/C ratio of 20%

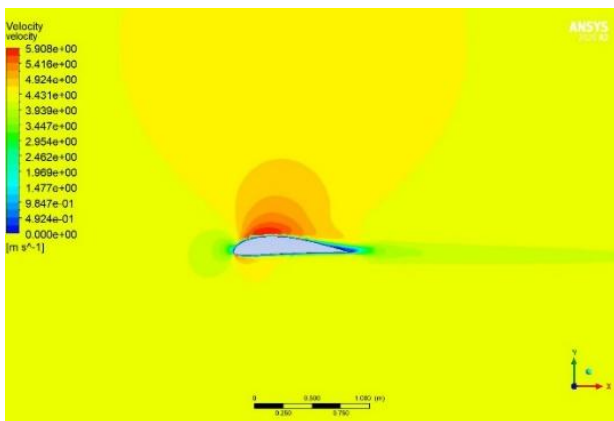


Figure 4: Velocity contour for t/C ratio of 5%

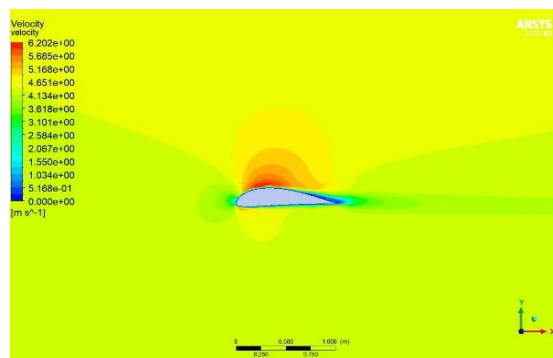


Figure 8: Velocity contour for t/C ratio of 25%

Based on the pictures above, contours around the airfoil can provide information on the airflow velocity distribution

based on the area's color around the airfoil. It can be seen that the maximum airflow velocity increases as the  $t/C$  ratio increases. In addition, it can be seen that the greater the airfoil  $t/C$  ratio, the wider the velocity distribution area with a relatively large value. The following is the simulation result with geometric parameters in the form of thickness-to-chord ratio with variations of 5%, 10%, 15%, 20%, and 25%.  $C_L$  is the lift coefficient,  $C_D$  is the drag coefficient, and  $C_L/C_D$  is the lift-to-drag ratio.

Table 2: Simulation Results for Various  $t/C$  ratio

	Thickness-to-Chord Ratio				
	5%	10%	15%	20%	25%
$C_L$	0.3854	0.4051	0.4681	0.4368	0.4468
$C_D$	0.0280	0.0243	0.0260	0.0352	0.0452
$C_L/C_D$	13.764	16.6708	18.0038	12.4091	9.8850

The airfoil with a thickness-to-chord ratio variation of 15% produced the largest lift-to-drag ratio compared to the other variations, which is 18.0038. Meanwhile, the airfoil that produces the smallest lift-to-drag ratio is the airfoil with a thickness-to-chord ratio of 25% compared to the other variations, which is 9.8850. The lift and drag coefficients from the simulation with geometric parameters in the thickness-to-chord ratio are shown in the figure below. These figures show that the greater the thickness-to-chord ratio of an airfoil geometry, the resulting lift coefficient tends to increase. Meanwhile, the greater the thickness-to-chord ratio of an airfoil, the resulting drag coefficient tends to grow as well.

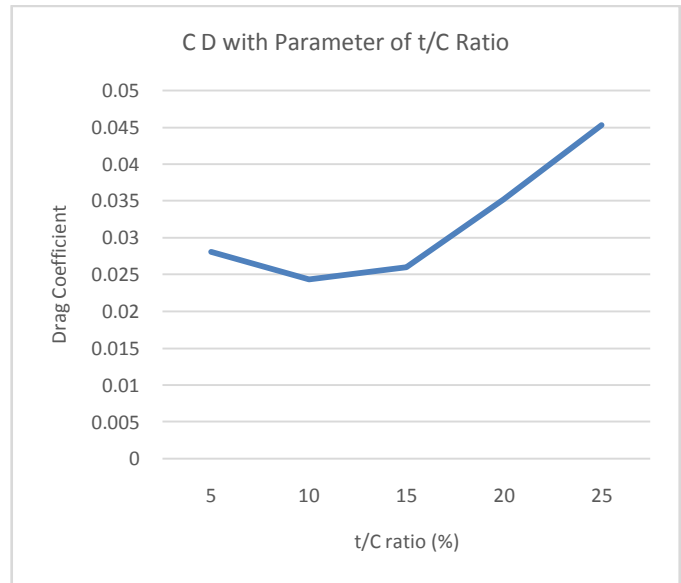


Figure 10:  $C_D$  for various  $t/C$  ratio

From the chord length parameter simulation, an overview of the airflow velocity conditions in the area around the airfoil is obtained with chord length variations of 1000 mm, 1250 mm, 1500 mm, 1750 mm, and 2000 mm with a fixed thickness. The contour of velocity from the simulation with geometric parameters in the form of chord length is shown in Figures 11 to 15.

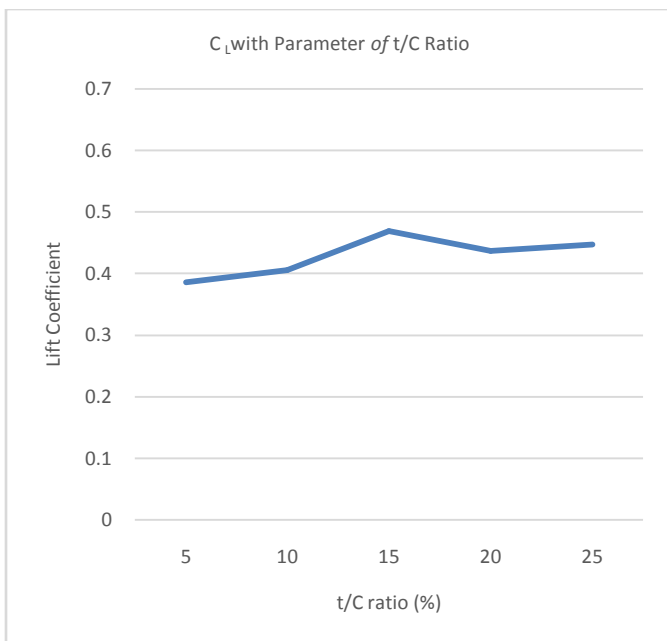


Figure 9:  $C_L$  with for various  $t/C$  ratio

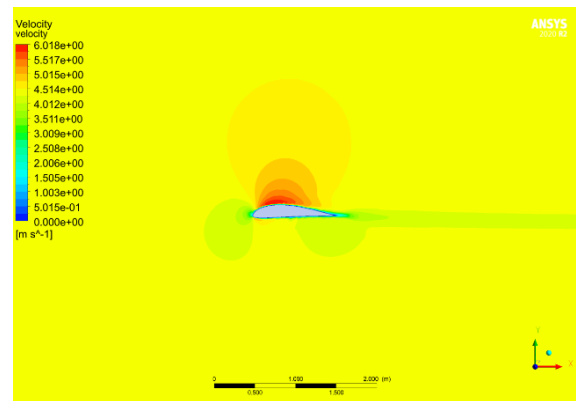


Figure 11: Velocity Contour for Chord Length of 1 m

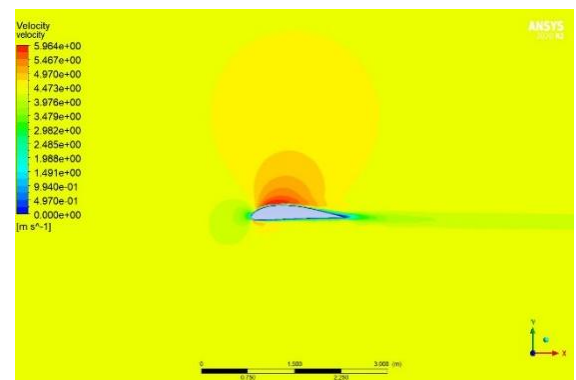


Figure 12: Velocity Contour for Chord Length of 1,25 m

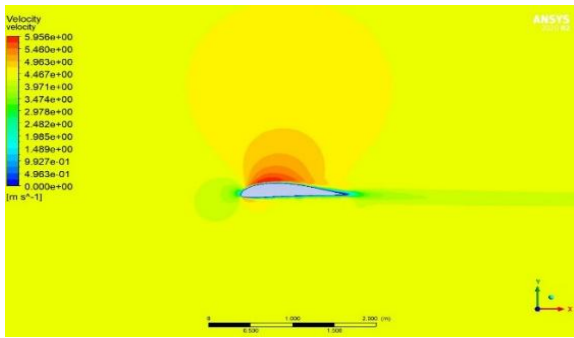


Figure 13: Velocity Contour for Chord Length of 1,5 m

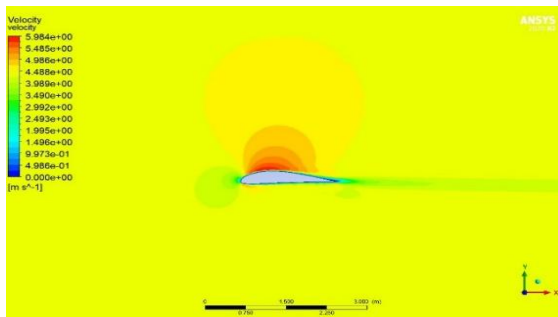


Figure 14: Velocity Contour for Chord Length of 1,75 m

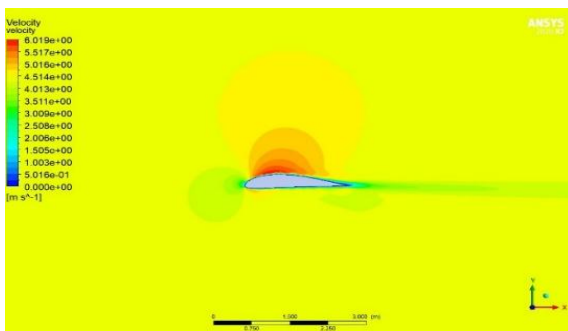


Figure 15: Velocity Contour for Chord Length of 2 m

Based on the pictures above, contours around the airfoil can provide information on the airflow velocity distribution based on the area's color around the airfoil. It can be seen that the maximum airflow velocity decreases with the increasing chord length of the airfoil. Also, the value of the maximum velocity of airflow around the airfoil tends to get smaller. The following are the results with geometric parameters of chord length with variations of 1000 mm, 1250 mm, 1500 mm, 1750 mm, and 2000 mm.

Table 3: Simulation Results with the Chord Length

	Chord Length				
	1000 mm	1250 mm	1500 mm	1750 mm	2000 mm
$C_L$	0.4799	0.4125	0.3942	0.4276	0.4231
$C_D$	0.0213	0.0239	0.0250	0.0224	0.0244
$C_L/C_D$	22.5305	17.2594	15.7680	19.0893	17.3402

The airfoil with a chord length variation of 1000 mm has the largest lift-to-drag ratio compared to the others by obtaining a  $C_L/C_D$  ratio of 22.5305. The airfoil that produces the smallest lift-to-drag ratio is the airfoil with a chord length of 15% compared to the other variations, which is 15.7680.

The graph of the lift and drag coefficients from the simulation results with geometric parameters in the form of chord length is shown in the figure below. The graph shows that the longer the chord on the airfoil, the resulting lift increases and decreases with a value difference that is not too big. In addition, the drag coefficient produced by the airfoil will increase and decrease each time the chord length increases.

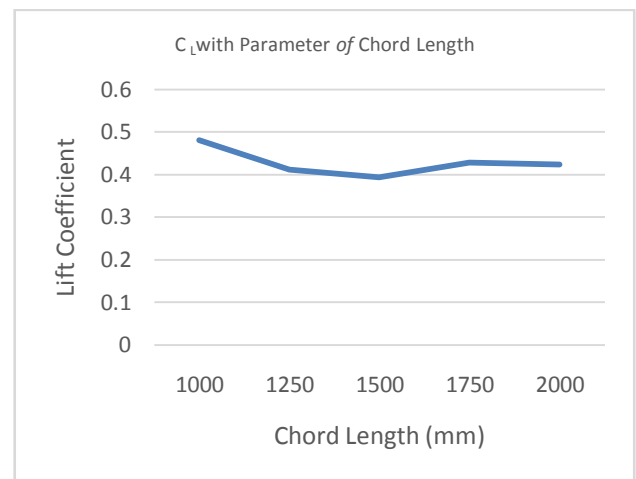


Figure 16:  $C_L$  for various Chord Length

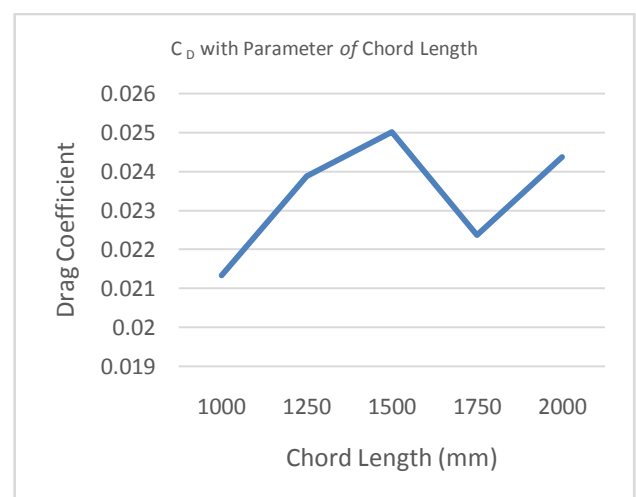


Figure 17:  $C_D$  for various Chord Length

Ghazijahani et al. [10] examined the effect of the thickness-to-chord ratio on the wing of a UAV (Unmanned Aerial Vehicle) on its aerodynamic characteristics. This research shows a higher lift coefficient ( $C_L$ ) when the ratio

$t/C$  increases at a low angle of attack. In this study, the lift coefficient values increased frequently with an increasing  $t/C$  ratio and a low angle of attack of  $0^\circ$ . The lift coefficient value obtained has increased at the  $t/C$  ratio of 5% to 15% with a value of 0.3854 to 0.4681. In addition, in Ghazijahani's study, an increase in the  $t/C$  ratio also caused a significant increase in  $C_D$  and a significant decrease in  $C_L/C_D$  value. In this study, the drag coefficient value experienced a considerable increase, namely at the  $t/C$  ratio of 5% to 25%, where the drag coefficient value obtained was 0.0243 and increased until it reached a value of 0.0452. Research conducted by Dongliet al. [14] examined the effect of the relative thickness of an airfoil on aerodynamic characteristics and showed a  $C_L/C_D$  ratio curve. There is a proportional decrease in the maximum lift-drag ratio due to the greater thickness value.

The data presented in the research table also shows that the greater the thickness-to-chord ratio of an airfoil, the lower the ratio of  $C_L/C_D$  will be. In addition, research conducted by Dhatchanamurthy et al. [15] confirmed that The maximum lift is achieved from certain airfoils when the maximum thickness-to-chord ratio ranges from 15% to 17%. The data presented in this study shows that the largest lift-to-drag coefficient, with a value of 18.0038, is obtained from an airfoil with a geometry with a thickness-to-chord ratio of 15%.

In the present study, the lift coefficient values increased and decreased with varied geometric parameters in chord length. The lift coefficient has increased on the airfoil with a chord length of 1750 mm from 1500 mm, which is 7,8%. This can be correlated with research conducted by Ghiyasi et al. [16], which examined four types of airfoils: symmetrical and asymmetrical. They noted that the longer chord lengths for wind turbines could provide higher power at lower blade tip speeds. This was the case in all four airfoil types selected. In addition, Pramono, Ambarita, and Kishinami [17] investigated the performance of an airfoil, which is affected by its chord length. From this research, it is known that non-dimensional chord length greatly affects strength. The greater the increase in chord length, the greater the resulting force.

## V. CONCLUSION

With the results from this study and the main literature, the validation calculation results are obtained with a difference value of 7.1682% or below 10%. This shows that this simulation calculation and the described aerodynamic characteristics have been validated with results close to the reference literature.

Based on the simulations in this study, it is shown that variations in chord length have an effect in the form of increases and decreases in the value of the lift coefficient and a decrease in the  $C_L/C_D$  ratio, which is caused by the

increasing value of the chord length of GOE-387 airfoil. In addition, variations in the thickness-to-chord ratio parameter also clearly influence the aerodynamic characteristics of GOE-387 airfoil. If the thickness-to-chord ratio of the airfoil is greater, there will be a significant increase in both the value of the lift coefficient and the drag coefficient while the  $C_L/C_D$  ratio decreases.

The suggestion for the development of this research in the future is to compare the effect of geometric parameters in this study between airfoils for aircraft wing applications and airfoils for blades in wind turbines. So that it can be seen the differences and similarities between the two airfoils under the influence of these geometric parameters.

## REFERENCES

- [1] Akbar, A. (2020). Effect of angle of attack on airfoil NACA 0012 performance, *REM Journal*, 5(1), pp. 35–40. doi:10.21070/remv5i1.1235.
- [2] Göv, İ. and Doğru, M.H. (2020). Aerodynamic optimization of NACA 0012 airfoil, *The International Journal of Energy & Engineering Sciences*, 5(2), pp. 146–155.
- [3] Akram, M.T. and Kim, M.H. (2021). CFD analysis and shape optimization of airfoils using class shape transformation and genetic algorithm, Part I, *Applied Sciences*, 11(9), pp. 1–23. doi:10.3390/app11093791.
- [4] Buyukluoğlu, Ö.F. and Bayram, H. (2015). Aerodynamic performance analysis of airfoils using the CFD method, *International Symposium on Sustainable Aviation*, pp.1-4.
- [5] Wozniak, J. (2021). Research and analysis of optimizing airfoil geometry and angle of attack to maximize short takeoff and landing capabilities, *Int. Journal of Engineering Research & Technology*, 10, pp. 462–467.
- [6] Othman, K.A. and Al-Obaidi, A.S.M. (2021). Effect of the wing airfoil shape on the aerodynamics and performance of a jet-trainer aircraft - an optimization approach, *Journal of Physics: Conference Series*, 2021 (1). doi:10.1088/1742-6596/2120/1/012011.
- [7] Hariyadi, S. (2017). An analysis on aerodynamics performance simulation of NACA 23018 airfoil wings on cant angles, *Journal of Energy, Mechanical, Materials, and Manufacturing Engineering*, 2(1), pp. 31–40. doi:10.22219/jemmm.v2i1.4905.
- [8] Khan, M.M.I. and Al-Faruk, A. (2018). Comparative analysis of aerodynamic characteristics of rectangular and curved leading edge wing planforms, *American Journal of Engineering Research (AJER)*, 7(5), pp. 281–291.
- [9] Yechout, T.R. et al. (2003). *Introduction to aircraft*

*flight mechanics: performance, static stability, dynamic stability, and classical feedback control.* Edited by J.A. Schetz, Virginia, American Institute of Aeronautics and Astronautics, Inc.

- [10] Ghazijahani, M.S. and Yavuz, M.M. (2019). Effect of thickness -to chord ratio on the aerodynamics of non-slender delta wing, *Aerospace Science and Technology*. doi:10.1016/j.ast.2019.03.033.
- [11] Budiprasojo, A. and Firmansyah, M.R. (2022). Aerodynamic analysis in designing an electric vehicle model tobacco style m-164 with computational fluid dynamic (CFD) method, *Mechanical Engineering Journal*, 13(2), pp . 435–442.
- [12] Reza, M.M.S., Mahmood, S.A. and Iqbal, A. (2016). Performance analysis and comparison of high lift airfoil for a low-speed unmanned aerial vehicle, *International Conference on Mechanical, Industrial and Energy Engineering 2016*. doi: 10.5281/zenodo.1468120.
- [13] Ogbeide, O.O. and Uwoghiren, G.O. (2022). Computational fluid dynamic (CFD) analysis of NACA airfoil for wind turbine blade design, *Industrial Engineering Letters*, 12(2), pp. 15–31. doi:10.7176/iel/12-2-03.
- [14] Dongli, M., Yanping, Z., Yuhang, Q., and Guanxiong, L. (2015). Effects of relative thickness on aerodynamic characteristics of airfoil at a low Reynolds number. *Chinese Journal of Aeronautics*, Vol. 28, Issue 4, pp. 1003-1015 doi: 10.1016/j.cja.2015.05.012.
- [15] Dhatchanamurthy, P., Gopinath, M. and Karthikeyan, L.M. (2014). A Study on the role of camber and thickness ratio on the airfoil characteristics using CFD software, *International Journal of Advanced Technology in Engineering and Science*, 2(12), pp. 611–623.
- [16] Ghiasi, P. et al.(2022). Analytical study of the impact of solidity, chord length, number of blades, aspect ratio, and airfoil type on h-rotor Darrius wind turbine performance at low Reynolds number, *Sustainability*, 14(2623), p. 14.doi:10.3390/su14052623.
- [17] Indro Pramono, Himsar Ambaritaand Koki Kishinami(2019). Effect of chord length on the performance of Darrius wind turbine with NACA 4415 airfoil. *IOP Conf. Ser.: Mater. Sci.Eng.* 648, 012030 doi 10.1088/1757-899X/648/1/012030.

**Citation of this Article:**

Nazaruddin Sinaga, Bambang Yuniato, Yosia Verse Pirie, “Effect of Thickness-to-Chord Ratio and Chord Length on Aerodynamics of GOE-387 Airfoil”, Published in *International Research Journal of Innovations in Engineering and Technology - IRJIET*, Volume 8, Issue 5, pp 280-287, May 2024. Article DOI <https://doi.org/10.47001/IRJIET/2024.805038>

\*\*\*\*\*